Malaria Journal

https://doi.org/10.1186/s12936-025-05743-6

Article in Press

Interactions between *Plasmodium falciparum* –infected red blood cells and their extracellular vesicles with megakaryocytes: implications for platelet-like particle formation

Received: 22 Oct 2025

Accepted: 11 Dec 2025

Published online: 18 December 2025

Cite this article as: Nunthanasup, N., Palasuwan, A., Palasuwan, D. *et al.* Interactions between *Plasmodium falciparum* –infected red blood cells and their extracellular vesicles with megakaryocytes: implications for platelet-like particle formation. *Malar J* (2025). https://doi.org/10.1186/s12936-025-05743-6

Nuntiporn Nunthanasup, Attakorn Palasuwan, Duangdao Palasuwan & Valery Combes

Title: Interactions between *Plasmodium falciparum*–infected red blood cells and their extracellular vesicles with megakaryocytes: Implications for platelet-like particle formation

Nuntiporn Nunthanasup[1], Attakorn Palasuwan[2], Duangdao Palasuwan[2]*, Valery Combes[3]*

[1]Programme in Clinical Hematology Sciences, Department of Clinical Microscopy, Faculty of Allied Health Sciences, Chulalongkorn University, Bangkok, Thailand

[2]Oxidation in red cell disorders research unit, Department of Clinical Microscopy, Faculty of Allied Health Sciences, Chulalongkorn University, Bangkok, Thailand

[3]Malaria and Microvesicles Research Group, School of Life Sciences, Faculty of Sciences, University of Technology Sydney, Sydney, Ultimo 2007, New South Wales, Australia

* Corresponding author's contact information

Duangdao Palasuwan, Ph.D., Oxidation in Red Cell Disorders Research Unit, Department of Clinical Microscopy, Faculty of Allied Health Sciences, Chulalongkorn University, Bangkok, Thailand. Email: nantadao@gmail.com Phone number: +6622181541 Fax number: +662183771

ORCiD https://orcid.org/0000-0003-3946-071X

Valery Combes, Associate Professor. Associate Head of School (Education & Students)

Microvesicles and Malaria Research Group Head, Faculty of Science | School of Life Sciences, Building 4, Room 04.06.424, University of Technology Sydney, Ultimo 2007, NSW, Australia.

Email: valery.combes@uts.edu.au Phone number: +61295144102

ORCiD https://orcid.org/0000-0003-2178-3596

Abstract

Background Thrombocytopenia commonly accompanies *Plasmodium falciparum* (*P. falciparum*) malaria, yet the role of impaired megakaryopoiesis and platelet production remains unclear. This study examined how *P. falciparum*–infected red blood cells (pRBCs) and their extracellular vesicles (EVs) modulate megakaryocytic differentiation and platelet-like particle (PLP) formation.

Methods MEG-01 cell line, a human megakaryoblastic leukaemia model, was differentiated with phorbol 12-myristate 13-acetate (PMA) in the presence or absence of fetal bovine serum (FBS) and co-cultured with pRBCs, normal RBCs (nRBCs), or their EVs (nRBC-EVs/pRBC-EVs). Changes in cell phenotype, adhesion, and gene expression were analyzed by flow cytometry, confocal microscopy, and qPCR. PLP functionality was assessed by clotting assays, and cytokine secretion was quantified using cytometric bead array.

Results pRBCs transiently adhered to MEG-01 cells but suppressed megakaryocytic marker expression, downregulated *NOTCH3*, and altered apoptosis- and stress-related genes. PLP production increased under some conditions, but clotting activity was impaired, indicating reduced functionality. In contrast, RBC-EVs, particularly pRBC-EVs, were internalized but induced minimal transcriptional or functional changes. Cytokine profiling revealed that pRBCs and their EVs selectively increased IL-8, RANTES, and MCP-1 levels.

Conclusions Intact pRBCs strongly inhibit megakaryocytic differentiation and disrupt PLP function through transcriptional dysregulation and inflammatory activation, whereas under our experimental conditions, RBC-EVs exert milder modulatory effects. These findings highlight defective platelet production as a novel mechanism contributing to malaria-associated thrombocytopenia.

Keywords Malaria, *Plasmodium falciparum*, thrombocytopenia, megakaryopoiesis, platelet-like particles, extracellular vesicles, red blood cell interactions

Background

Severe malaria, primarily caused by *P. falciparum*, remains a major cause of morbidity and mortality in tropical regions. Thrombocytopenia is one of the most consistent haematological manifestations of malaria and is associated with increased bleeding risk, disease severity, and poor clinical outcomes (1, 2). The mechanisms underlying malaria-induced thrombocytopenia are multifactorial and include platelet destruction, splenic sequestration, and potentially impaired platelet production in the bone marrow (BM) (2-4). However, the contribution of defective megakaryopoiesis, the process by which megakaryocytes (MKs) mature and release platelets, remains insufficiently understood (5, 6). Disruption of MK differentiation or platelet formation could therefore play a key role in the observed platelet depletion during malaria infection.

EVs are nanosize, membrane-bound particles released by virtually all cell types and are increasingly recognized as important mediators of intercellular communication and immune modulation (7, 8). In malaria, pRBC-EVs contribute to host–parasite interactions and disease pathogenesis (9-11). These vesicles can transfer parasite components, including proteins and RNA, to host cells, thereby influencing immune responses, inflammation, and vascular function (12-16). Elevated levels of circulating pRBC-EVs have been reported in malaria patients and correlate with disease severity and immune activation (12, 17-19). Importantly, EVs have been shown to stimulate cytokine release from monocytes and endothelial cells, promoting systemic inflammation (16). Experimental evidence also suggests that these vesicles may affect

haematopoietic and megakaryocytic processes within the BM (20), yet their specific role in regulating MK maturation and platelet biogenesis remains poorly defined.

Megakaryopoiesis and platelet production are tightly regulated by cytokines and signalling pathways, including thrombopoietin, interleukins, and stem cell factor (21, 22). Pathways such as Notch signalling and platelet-derived growth factor (PDGF) receptor signalling are also essential for MK maturation and platelet release (23, 24). Disruption of these pathways during malaria infection could therefore lead to defective thrombopoiesis. Moreover, both platelet activation and inflammatory cytokine imbalance have been implicated in the haematological abnormalities associated with severe malaria (4, 25-27).

The MEG-01 cell line, a human megakaryoblastic leukaemia model, provides a robust *in vitro* system for studying megakaryocytic differentiation and PLP formation (28). Using this model, we investigated the effects of pRBCs and their EVs on MK maturation and PLP generation. We optimized differentiation conditions using PMA and FBS to enhance PLP formation, and subsequently co-cultured MEG-01 cells with pRBCs or pRBC-EVs to assess their impact on megakaryocytic phenotype, gene expression, cytokine secretion, and PLP functionality.

In summary, this study explores how *P. falciparum* infection and its associated EVs modulate MK differentiation and platelet production. We demonstrate that intact pRBCs, more than their EV counterparts, inhibit megakaryocytic maturation and impair PLP functionality, providing mechanistic insight into the pathogenesis of malaria-associated thrombocytopenia.

Methods

Maintenance of the MEG-01 cell line

The human megakaryoblastic cell line MEG-01 (Merck Life Science, Australia) was maintained in RPMI-1640 medium (Thermo Fisher Scientific, USA) supplemented with 10% heat-inactivated FBS. Cells were cultured at 37 °C in a humidified incubator with 5% CO_2. For subculture, cells were gently detached using a 25-cm cell scraper (Sarstedt, Inc., Newton, NC, USA). For morphological assessment, 22-mm^2 glass coverslips were placed in 6-well plates, and MEG-01 cells were seeded at 5×10^5 cells/ml.

Differentiation and generation of PLPs

To induce megakaryocytic differentiation and evaluate PLP formation, MEG-01 cells were cultured with or without FBS and stimulated with or without 50 ng/ml PMA (EMD Millipore Corporation, USA) under four conditions: +FBS/−PMA, −FBS/−PMA, −FBS/+PMA, and +FBS/+PMA. PMA is a potent activator of protein kinase C (PKC) that promotes megakaryocytic maturation, adhesion, and proplatelet formation, while the presence or absence of FBS allows evaluation of serum-dependent survival and differentiation cues. Cells were incubated at 37 °C for five days. Following centrifugation at 150 × g for 5 min, cells were collected, and the supernatant was centrifuged at 500 × g for 10 min to obtain PLP pellets. Both MEG-01 cells and PLPs were washed with phosphate-buffered saline (PBS) and stained with fluorochrome-conjugated antibodies against CD41a, CD42b, and CD61 (canonical megakaryocytic markers reflecting integrin αIIbβ3 and GPIb expression), Notch3 (a regulator of MK proliferation and differentiation), and Annexin V (to detect early apoptosis). These markers were chosen to evaluate both maturation and viability status during differentiation. Samples were analyzed on a CytoFLEX S flow

cytometer (Beckman Coulter, USA), and PLPs were identified based on forward and side scatter profiles comparable to those of human platelets.

P. falciparum culture

P. falciparum 3D7 strain was maintained at 5% hematocrit in complete medium composed of RPMI-1640 supplemented with 10 μM hypoxanthine, 0.5% w/v Albumax II® (BSA lipid-rich), 10 mM D-glucose, and 20 μg/ml gentamicin. Cultures were incubated at 37 °C under a gas mixture of 5% O_2, 5% CO_2, and 90% N_2. Parasitemia was expanded to 25–30% using O^+ human red blood cells (Australian Red Cross Lifeblood, Sydney). Although *in viv*o parasitemia in malaria patients is typically lower due to sequestration of mature stages in the microvasculature, high *in vitro* parasitemia was used to ensure sufficient interaction between pRBCs and MEG-01 cells. This approach is consistent with previous *in vitro* studies achieving 20–30% parasitemia for synchronized cultures (29). After culture, samples were centrifuged at 500 × g for 5 min, and supernatants were collected for EV purification.

Isolation of EVs from RBCs and pRBCs

Supernatants from nRBC and pRBC cultures were centrifuged twice at 20,000 × g for 5 min to remove debris. The clarified supernatant was further ultracentrifuged twice at 150,000 × g for 90 min (Optima MAX-TL, Beckman Coulter, USA). Pellets were gently resuspended in 20-50 μl DPBS and stored at 4 °C for short-term use. All isolation steps were performed according to the MISEV 2023 guidelines to minimize contamination from protein aggregates, hemozoin, and other non-vesicular components. The number of EVs added to MEG-01 cultures was standardized across

all experiments (2×10^{10} EV particles per 10^5 MEG-01 cells), ensuring comparable exposure regardless of the total yield obtained from RBC or pRBC preparations.

Characterization of EV concentration and size

Particle concentration and diameter were determined using nanoparticle tracking analysis (NTA; ZetaView QUATT, Particle Metrix, Germany). Samples were diluted in 0.2-μm filtered DPBS (1:2,000–1:8,000) to achieve optimal particle counts (50–200 particles/frame, sensitivity 85). Each sample was analyzed in triplicate, and 0.2-μm DPBS served as a blank control.

Fluorescent labeling of EVs

Purified EVs were stained with PKH26 (Sigma-Aldrich, USA) following the manufacturer's instructions. Briefly, 250 μl of EV suspension was mixed with 1 μl PKH26 dye in 250 μl DPBS and incubated for 5 min at room temperature. Staining was quenched by adding 500 μl FBS. Samples were incubated overnight in RPMI + 10% FBS at 37 °C, centrifuged at 150,000 × g for 90 min, and resuspended in 20–50 μl DPBS. Fluorescence was confirmed by flow cytometry (PE channel, CytoFLEX S).

Co-culture of MEG-01 cells with RBCs or EVs

MEG-01 cells were cultured under −FBS/+PMA or +FBS/+PMA conditions and co-incubated with either pRBCs or their EVs to examine malaria-related effects on megakaryocytic differentiation and PLP formation. A parasitemia level of 25–30% was deliberately used to ensure sufficient exposure of MEG-01 cells to pRBCs, consistent with the culture expansion described in Section 2.3 and reflecting the high parasite burdens typically found within tissue

microenvironments such as the BM, where sequestration leads to higher local parasite density than in circulating blood (30-32). For co-culture, MEG-01 cells were incubated with pRBCs (25–30% parasitemia) or with 2×10^{10} EV particles per 10^5 MEG-01 cells for 5 days. nRBCs and nRBC-EVs served as negative controls. After incubation, both MEG-01 cells and released PLPs were collected, washed with PBS, stained with fluorochrome-conjugated antibodies, and analyzed by flow cytometry.

Binding assays and imaging

For fluorescence-based binding assays, MEG-01 cells were pre-stained with 1× CellTracker™ Deep Red Dye (CTDR; Thermo Fisher Scientific, USA) for 45 min at 37 °C, while pRBCs were labeled with 5 μM Hoechst and PKH26. Co-cultures were prepared at 50 RBCs per MEG-01 cell or 2×10^{10} EVs per 10^5 MEG-01 cells and incubated for 5 h or overnight (~18 h). Binding was quantified by flow cytometry and confocal microscopy (Nikon A1R HD25, 40× objective). For z-stack analysis, 0.25 μm optical slices were acquired and analyzed using NIS-Elements and ImageJ.

Cytokine quantification

Supernatants collected on days 3 and 5 were analyzed for IL-8, MIP-1α, RANTES, and MCP-1 using the BD Cytometric Bead Array (CBA) Human Soluble Protein Master Buffer Kit, following the manufacturer's instructions (BD Biosciences, USA). Data were acquired on a BD LSRFortessa™ X-20 and analyzed using BD® CBA Analysis Software.

Quantitative real-time PCR

Total RNA was extracted using TRIzol (Thermo Fisher Scientific, USA) and reverse-transcribed to cDNA using iScript™ Reverse Transcription Supermix (Bio-Rad, USA). qPCR was performed using PowerUp™ SYBR™ Green Master Mix (Thermo Fisher Scientific) on a QuantStudio 12K Flex system. Primers (Integrated DNA Technologies) for DLL4, NOTCH3, PDGFRB, BAX, BCL2, CASPASE3, CASPASE9, ATG7, MTOR, and NOX1 are listed in Table 1. Expression was normalized to GAPDH and analyzed by the $2^{-\Delta\Delta CT}$ method. Biological replicates: n = 3 independent experiments.

PLP functional assay (plasma clotting time)

The functional activity of PLPs was evaluated by thrombin-induced clotting assay. Platelet-poor plasma (PPP, 0.1-μm filtered) and 25 mM $CaCl_2$ were mixed with PLP-containing supernatants at 37 °C. Clot formation time was recorded as the interval from mixing to fibrin gel formation. Platelet-rich plasma (PRP) and PPP served as positive and negative controls, respectively.

Statistical analysis

Graphs were generated using GraphPad Prism 9.5.0 and data analyzed with SPSS SigmaStat 28.0.0.0. Results are presented as mean ± SD. Comparisons between groups were performed using one-way ANOVA followed by Bonferroni post hoc tests or Student's t-test as appropriate. Significance levels are noted with * for $p < 0.05$, ** for $p < 0.01$, *** for $p < 0.005$, and **** for $p < 0.001$, whereas # $p < 0.05$, ## $p < 0.01$, ### $p < 0.005$, and #### $p < 0.001$ indicate comparisons within the same condition but on different days.

Ethics approval

All procedures complied with the Declaration of Helsinki and ICH-GCP guidelines. Ethical approval was obtained from the Chulalongkorn University Ethical Review Committee (COA No. 186/67), the University of Technology Sydney Human Research Ethics Committee (ETH20-5280), and the Australian Red Cross Lifeblood Ethics Committee (ETH24-9504). Human blood products were obtained from de-identified donations; written informed consent was not required under the approved protocols.

Results

Experimental design for PLP generation from MEG-01 cells and validation of RBC-EVs

MEG-01 cells were cultured under four differentiation conditions (+FBS/−PMA, −FBS/−PMA, −FBS/+PMA, +FBS/+PMA) to identify optimal parameters for PLP generation. Surface marker expression, PLP yield, clotting function, and cytokine secretion were analyzed on days 3 and 5. Following optimization, MEG-01 cells were co-cultured with either nRBCs or pRBCs (25–30% parasitemia) and their corresponding EVs to assess malaria-related effects (Fig. 1a). The integrity of isolated EVs was confirmed by PKH26 staining and flow cytometry (PBS blank), showing clear PKH26-positive populations and strong linearity across serial dilutions ($R^2 = 0.9976$ for nRBC-EVs; $R^2 = 0.9982$ for pRBC-EVs; Additional file 1, Fig. S1a–b). NTA indicated mean diameters of 171.8 ± 6.1 nm (median 156.3 ± 7.9 nm) for nRBC-EVs and 162.2 ± 26.4 nm (median 149.1 ± 18.2 nm) for pRBC-EVs (Additional file 1, Fig. S1c). The average yield was in the range of 10^{11} particles/mL for both EV types (Additional file 1, Fig. S1d). Overall, these data confirm successful EV recovery and establish the experimental framework for downstream co-culture assays.

FBS and PMA synergistically increase MEG-01 adhesion; pRBCs induce a transient adhesive response while RBC-EVs have minimal effect

Microscopy and quantitative analysis demonstrated that both FBS and PMA markedly promote MEG-01 adhesion and PLP release (Fig. 1b–c). The +FBS/+PMA condition produced the highest adhesion (61.3% on day 5 vs 9.2% on day 3; ****$p < 0.001$, ####$p < 0.001$). Serum deprivation abolished adhesion irrespective of PMA. Co-culture with nRBCs or pRBCs (25–30% parasitemia) produced visible RBC binding to MEG-01 cells in both −FBS/+PMA and +FBS/+PMA settings (Fig. 1d, f). Under −FBS/+PMA, pRBCs transiently increased adhesion (ratio = 2.75 on day 3; **$p < 0.01$) but this effect resolved by day 5 (ratio = 0.98; ##$p < 0.01$) (Fig. 1e). A similar transient effect occurred under +FBS/+PMA (day 3 ratio = 2.36; ****$p < 0.001$ to day 5 ratio = 0.63; ####$p < 0.001$) (Fig. 1g). By contrast, co-incubation with nRBC-EVs or pRBC-EVs (10^{10} particles/10^5 MEG-01) produced no substantial microscopic changes in adhesion; only a minor increase with pRBC-EVs on day 5 (#$p < 0.05$) was observed, indicating minimal overall EV impact on adhesion (Additional file 1, Fig. S2a−c).

Time-dependent interactions measured by flow cytometry: stronger overnight binding, distinct patterns for RBCs versus RBC-EVs

For clarity, “RBC” refers to either nRBC or pRBC, while “RBC-EVs” denotes EVs derived from each respective source. Both adherent and floating fractions of MEG-01 cells were analyzed separately, representing attached, differentiated cells and those in suspension, less mature cells, respectively. Flow cytometry revealed time-dependent increases in MEG-01 interactions with RBCs or RBC-EVs, with differences between adherent and floating subpopulations (Fig. 2d–f; Additional file 1, Fig. S5). At 5 h, interactions were low and similar across groups. Overnight

incubation markedly increased interactions for both adherent and floating cells (####$p < 0.001$). Adherent MEG-01 showed larger overnight increases with nRBCs ($\Delta = 26.13\%$) than with pRBCs ($\Delta = 10.33\%$), and nRBC binding exceeded pRBC binding (****$p < 0.001$; Fig. 2e). By contrast, EV-mediated binding behaved differently: pRBC-EVs displayed greater binding than nRBC-EVs at 5 h (adherent $\Delta = 2.84\%$; floating $\Delta = 2.40\%$) and this divergence expanded overnight (adherent $\Delta = 10.41\%$; floating $\Delta = 8.77\%$) (****$p < 0.001$, ####$p < 0.001$; Fig. 2f). Thus, intact nRBCs promote more pronounced cell–cell contact overnight, whereas pRBC-EVs show stronger vesicle-mediated engagement over time.

Confocal microscopy confirms surface association of intact RBCs and internalization of RBC-EVs after overnight exposure

Confocal imaging with z-stack analysis corroborated flow cytometry findings. Both nRBCs and pRBCs adhered to MEG-01 cells at 5 h and overnight but remained surface-associated (no internalization detected) (Fig. 2a, c; Additional file 1, Fig. S3a, c). Overnight binding increased significantly versus 5 h, and nRBCs associated more strongly than pRBCs (40.8% difference; ****$p < 0.001$; Fig. 2b). In contrast, nRBC-EVs and pRBC-EVs were observed both on the surface and internalized within MEG-01 cells after overnight incubation, as shown by z-stacks (Fig. 2c; Additional file 1, Fig. S3b, d). EV binding increased significantly overnight for both EV types (####$p < 0.001$). Similar patterns were present in floating cell fractions (Additional file 1, Fig. S4). Collectively, microscopy supports a model in which intact RBCs predominantly adhere to the MEG-01 surface, while RBC-EVs can be internalized upon prolonged exposure.

Intact RBCs suppress megakaryocytic surface marker expression on MEG-01 cells; EVs exert limited effects

Under PMA stimulation, particularly with FBS, MEG-01 cells upregulated canonical megakaryocytic markers (CD41a, CD42b, CD61), double-positive populations ($CD41a^+CD42b^+$, $CD41a^+CD61^+$) and Notch3 (Fig. 3a–g; Additional file 1, Figs S6a–b and S7a–g). However, co-culture with nRBCs or pRBCs under −FBS/+PMA or +FBS/+PMA substantially reduced expression of these markers, including double-positive subsets and Notch3, indicating that intact RBCs impair megakaryocytic maturation (Fig. 3h–n; Additional file 1, Figs S6c–d and S7h–n). Although the reduction in marker detection could partly reflect steric hindrance caused by adherent RBCs masking surface antigens, the consistent decrease across multiple markers, including Notch3, suggests true suppression of differentiation rather than a purely physical artifact. Annexin V expression remained largely unchanged across conditions, suggesting that apoptosis was not the primary driver of the observed differences. Exposure to nRBC-EVs or pRBC-EVs produced minimal changes in marker expression overall (Additional file 1, Figs S6e–f and S7o–u). The only consistent EV effect was a reduction of CD42b under −FBS/+PMA (****$p < 0.001$) and modest time-dependent declines of CD41a/CD42b between days 3 and 5 in EV-treated groups (####$p < 0.001$). These data indicate that direct contact with intact RBCs, rather than EVs, is the primary driver of megakaryocytic marker suppression.

pRBCs reduce megakaryocytic marker expression on MEG-01-derived PLPs; EVs have negligible influence

PLPs harvested from MEG-01 cultures under ±FBS and ±PMA exhibited expected platelet marker expression when differentiated (Fig. 4a–g; Additional file 1, Figs S8a–b and S9a–g). Co-culture

with pRBCs produced a pronounced reduction in PLP surface markers under both −FBS/+PMA and +FBS/+PMA, consistent with impaired PLP maturation (Fig. 4h–n; Additional file 1, Figs S8c–d and S9h–n). Notably, Notch3 was reduced in PLPs on day 3 under +FBS/+PMA when co-cultured with either pRBCs or nRBCs; Annexin V did not differ across groups. Co-culture with nRBC-EVs or pRBC-EVs elicited no significant changes in PLP marker profiles (Additional file 1, Figs S8e–f and S9o–u). Thus, intact pRBCs suppress phenotypic maturation of released PLPs, whereas EVs exert little effect.

pRBCs increase PLP yield but impair PLP clotting function under optimized conditions

PLP counts (per 5×10^5 MEG-01 cells) varied with culture conditions and co-culture components (Fig. 5a–c). On day 3, −FBS cultures produced fewer PLPs than +FBS/−PMA controls, whereas +FBS/+PMA yielded comparable counts to controls. By day 5, PLP numbers increased in all groups (day effect, ####$p < 0.001$; Fig. 5a). Co-culture with pRBCs increased PLP yield under −FBS/+PMA and +FBS/+PMA on both days (Fig. 5b). pRBC-EVs modestly increased PLP counts at day 5 under +FBS/+PMA but had little effect under −FBS/+PMA (Fig. 5c). Functionally, PLPs shortened clotting time relative to PPP (negative control) on day 3 and approached PRP (positive control) by day 5, indicating functional competency (Fig. 5d). However, PLPs generated in the presence of pRBCs exhibited significantly prolonged clotting times compared with nRBCs and controls (****$p < 0.001$) in both −FBS/+PMA and +FBS/+PMA conditions (Fig. 5e), indicating that pRBC exposure reduces PLP procoagulant function despite sometimes increasing PLP numbers. pRBC-EVs increased PLP counts without measurably altering clotting times.

Effects of serum, PMA, and RBC co-culture on gene expression: dynamic regulation of differentiation, apoptosis, and stress pathways

We profiled expression of 10 genes implicated in MK differentiation, apoptosis, and cellular stress on day 5 (DLL4, NOTCH3, PDGFRB, BAX, BCL2, CASPASE3, CASPASE9, ATG7, MTOR, NOX1; Fig. 6; Additional file 1, Figs S10–S11). Across baseline conditions, serum deprivation and absence of PMA modulated these transcripts in a context-dependent manner. PMA exposure tended to induce apoptotic markers (CASPASE3/9) and alter stress-related genes, whereas absence of PMA (and in some cases −FBS) was associated with higher DLL4, PDGFRB, and NOX1 in specific comparisons. (Fig. 6a–j; Additional file 1, Fig. S10a–j). Co-culture with intact nRBCs or pRBCs produced marked transcriptional changes: overall, several differentiation- and stress-related genes (including DLL4, PDGFRB, and NOX1) were substantially altered relative to +FBS/−PMA baseline, with many comparisons showing decreased expression by day 5 after co-culture (Fig. 6k–t; Additional file 1, Fig. S10k–t). NOTCH3 responses were context-dependent: modest elevations occurred under some co-culture conditions, whereas pRBC co-culture in +FBS/+PMA reduced NOTCH3 relative to +FBS/+PMA alone. Apoptosis-related transcripts (BAX, CASPASE9) showed transient increases under −FBS/+PMA but were often attenuated after prolonged co-culture with pRBCs. ATG7 and MTOR displayed modest, condition-dependent regulation, with some elevation in nRBC co-cultures consistent with metabolic adaptation. Overall, intact RBCs exert stronger and more sustained transcriptional modulation than RBC-EVs. RBC-EVs induced only minor and transient transcriptional changes: several genes (NOTCH3, CASPASE9, and others) were modestly reduced at early time points in +FBS/+PMA + EV co-culture (Additional file 1, Fig. S11a–j), but most effects resolved by day 5. Thus, EVs exert substantially weaker transcriptional influence than intact RBCs.

Distinct regulation of inflammatory cytokines by RBCs and RBC-EVs in PMA-stimulated MEG-01 cultures

Cytokine profiling (IL-8, MIP-1α, MCP-1, RANTES) revealed that PMA stimulation, particularly in +FBS/+PMA, elevates pro-inflammatory cytokine secretion compared with +FBS/−PMA (Fig. 7a–d; Additional file 1, Fig. S12a–d). Co-culture with nRBCs and pRBCs further increased IL-8, MIP-1α, MCP-1, and RANTES on day 3 versus −FBS/+PMA controls, with some reductions by day 5 (Fig. 7e–h; Additional file 1, Fig. S12e–h). EV addition produced selective cytokine modulation: under −FBS/+PMA, both nRBC-EVs and pRBC-EVs increased cytokine levels on day 3; under +FBS/+PMA, only MCP-1 remained elevated with EVs. By day 5, EV-driven differences were modest (Fig. 7i–l; Additional file 1, Fig. S12i–l). Collectively, intact RBCs induce a robust but transient cytokine response in differentiating MEG-01 cells, whereas RBC-EVs produce milder, more selective cytokine changes.

Discussion

Thrombocytopenia is a well-recognized hematologic complication of *P. falciparum* malaria and frequently correlates with disease severity and poor clinical outcomes (2, 30). While peripheral platelet consumption, splenic sequestration, and immune-mediated destruction are established contributors (4, 25), our findings suggest an additional mechanism: the suppression of megakaryopoiesis and platelet production by pRBCs and their EVs. Using the MEG-01 model, we demonstrated that intact pRBCs markedly inhibit megakaryocytic differentiation and impair PLP function, whereas RBC-EVs exert only modest and transient effects. These results highlight a dual

mechanism in malaria-associated thrombocytopenia, defective platelet production in addition to peripheral consumption.

Optimization experiments revealed that MEG-01 cells cultured with PMA and FBS exhibit enhanced adhesion, maturation, and PLP release. PMA serves as a potent activator of PKC, driving megakaryocytic differentiation and proplatelet formation (33-35), while FBS provides essential growth and adhesion factors that support survival and maturation (36, 37). These conditions were incorporated into the experimental design to evaluate how infected erythrocytes and their EVs might disrupt both survival-dependent and signalling-driven maturation pathways. Notably, serum-free conditions were included to mimic nutrient-limited environments, as serum deprivation is known to induce apoptosis and stress responses in hematopoietic progenitors. Although some studies have explored serum-free megakaryopoiesis (38, 39), FBS supplementation remains essential for optimal PLP yield in MEG-01 cultures.

Interestingly, co-culture with pRBCs led to an apparent paradox: an increased number of PLPs but with diminished functionality. This phenomenon may represent a stress-induced or abortive differentiation process rather than efficient thrombopoiesis. Supporting this, gene expression analysis revealed upregulation of autophagy-related ATG7, imbalance between pro- and anti-apoptotic genes (BAX/BCL2), and activation of metabolic stress regulators such as MTOR and NOX1. These findings are consistent with reports that oxidative and apoptotic stress can drive premature release of immature platelets with reduced hemostatic potential (39, 40).

The relatively high parasitemia level (25–30%) employed in this study was intentional. *In vivo*, peripheral parasitemia typically underestimates the true parasite burden because mature infected erythrocytes sequester in microvascular and BM compartments, where densities are markedly higher than in circulation (31, 32, 41). Thus, the chosen parasitemia more accurately reflects these

tissue conditions and ensures robust exposure of MEG-01 cells to parasite-derived factors. This also guarantees that a large proportion of EVs in pRBC cultures originate from infected cells, carrying surface and molecular signatures representative of their parasitic origin.

It is also possible that pRBC-EVs in this study exerted limited effects because their molecular cargo, particularly virulence-associated proteins, may differ from those found in microvesicles generated *in vivo* or during later parasite stages. This could explain their minimal impact compared to intact pRBCs, which directly contact and suppress megakaryocytic differentiation.

Mechanistically, we observed transient activation of the Notch signalling pathway, particularly through Notch3, in MEG-01 cells early after exposure to pRBCs. Notch signalling is known to govern MK lineage commitment and proplatelet formation (23, 42). The early but unsustained activation of NOTCH3 suggests that pRBC exposure may trigger an initial differentiation cue followed by signalling disruption, resulting in incomplete maturation. In contrast, RBC-EVs elicited only mild or transient modulation of Notch3 expression, reinforcing that direct cellular interactions, rather than vesicular cargo, are the dominant modulators of megakaryocytic signalling.

Confocal imaging further demonstrated that both nRBCs and pRBCs adhered to MEG-01 cells, yet only EVs were internalized. Notably, nRBCs exhibited stronger physical binding but caused minimal suppression of differentiation, suggesting that parasite-specific surface proteins, such as PfEMP1 or altered lipid composition, may underlie the inhibitory effect of pRBCs (8, 10, 15). EV internalization, on the other hand, may deliver signalling molecules without triggering the same level of suppression, consistent with their limited phenotypic impact observed in this study.

Cytokine profiling provided additional insight into the inflammatory context of these interactions. pRBCs induced elevated levels of IL-8 and MIP-1α, pro-inflammatory mediators linked to

leukocyte recruitment and tissue damage, whereas nRBCs enhanced MCP-1 and RANTES, associated with reparative or anti-inflammatory processes (26, 27). Such differential cytokine profiles suggest that *P. falciparum* infection skews megakaryocytic responses toward a pro-inflammatory state, potentially exacerbating platelet dysfunction and ineffective thrombopoiesis. Moreover, PMA itself promotes cytokine release through PKC-dependent pathways (9), which could further potentiate these inflammatory effects when combined with parasite-derived stimuli.

Several limitations of this study must be acknowledged. First, the MEG-01 cell line, while valuable for modeling megakaryocytic differentiation (28, 34), may not fully replicate the behavior of primary BM MKs, particularly in terms of ploidy, morphology, and responsiveness to cytokines. Second, the *in vitro* system lacks the stromal, immune, and extracellular matrix components of the native BM microenvironment. Third, while our EV isolation and characterization confirmed particle size and concentration, the molecular composition of these vesicles, including specific protein, RNA, or lipid cargo, remains to be determined. In addition, the use of a single EV dose precludes evaluation of concentration-dependent effects, and our functional analyses were limited to plasma clotting assays without assessing other platelet functions such as aggregation, adhesion, or activation. Moreover, PMA provides a robust but non-physiological stimulus, which may amplify differentiation signals differently from endogenous pathways. Finally, gene expression analyses focused on a selected panel of targets, and broader transcriptional profiling would likely yield deeper mechanistic insights.

Beyond these considerations, the interpretation of EV-specific effects requires further consideration. The EVs used in this study were generated under standard *in vitro* culture conditions for *P. falciparum* parasites, which do not replicate the cellular, biochemical, and mechanical complexity of the BM microenvironment. Because EV cargo composition is highly influenced by

microenvironmental cues, the vesicles examined here may differ from those produced *in vivo* during parasite–MK interactions (43, 44). Furthermore, EVs in this study were generated in the absence of reciprocal signalling from MKs. Although direct evidence for MK-driven modulation of RBC vesiculation is currently lacking, vesiculation of erythrocytes is known to be influenced by interactions with other cell types, such as endothelial cells and monocytes, which can alter membrane stability and promote vesicle release (45, 46). These observations support the broader concept that heterotypic cellular interactions can regulate RBC-EV production, though the relevance of such mechanisms to MK–pRBC crosstalk remains to be determined. Lastly, a more informative approach would involve isolating EVs directly from pRBC–MEG-01 co-cultures and assessing their effects on naïve MKs to determine whether "educated" EVs contribute to suppression of megakaryopoiesis.

Future investigations should aim to address these limitations by employing more physiologically relevant systems. Studies utilizing primary human MKs or induced pluripotent stem cell–derived megakaryocytic models will be critical for validating the *in vitro* mechanisms identified here. Systematic analysis of dose-dependent and stage-specific responses to *P. falciparum*–infected erythrocytes and their EVs could delineate threshold effects and dynamic signalling changes during differentiation. Implementation of EV-TRACK–compliant isolation protocols with standardized marker validation and detailed proteomic and transcriptomic profiling will enhance experimental rigor and comparability across studies. Expanding global transcriptomic analyses would also provide a comprehensive understanding of the gene networks governing differentiation, apoptosis, and stress adaptation. Lastly, *in vivo* models are needed to confirm whether impaired thrombopoiesis directly contributes to malaria-associated thrombocytopenia and

to evaluate potential therapeutic strategies targeting megakaryocytic stress and signalling pathways.

Conclusion

This study indicates that pRBCs can suppress megakaryocytic maturation and reduce PLP functionality in the MEG-01 model, likely through contact-dependent effects involving dysregulated Notch-related and stress-response pathways. In contrast, RBC-EVs were internalized but exerted comparatively modest transcriptional and functional effects under the experimental conditions used. Taken together, these findings support a contributory role of impaired platelet production, alongside platelet consumption, in the development of malaria-associated thrombocytopenia. By pinpointing the signalling and stress pathways that are altered during parasite–megakaryocyte interactions, this work provides a basis for exploring strategies that modulate megakaryopoiesis or protect platelet biogenesis in the context of severe malaria.

List of abbreviations

ANOVA	Analysis of variance
ATG7	Autophagy-related gene 7
BAX	Bcl-2–associated X protein
BCL2	B-cell lymphoma 2
BM	Bone marrow
BSA	Bovine serum albumin
CBA	Cytometric bead array
$CaCl_2$	Calcium chloride

CD41a	Platelet glycoprotein IIb (integrin αIIb)
CD42b	Platelet glycoprotein Ib alpha chain (GPIbα)
CD61	Platelet glycoprotein IIIa (integrin β3)
CO_2	Carbon dioxide
Ct	Cycle threshold
CTDR	CellTracker™ Deep Red Dye
DLL4	Delta-like canonical Notch ligand 4
DPBS	Dulbecco's phosphate-buffered saline
EVs	Extracellular vesicles
FBS	Fetal bovine serum
GAPDH	Glyceraldehyde-3-phosphate dehydrogenase
IL-8	Interleukin-8
MCP-1	Monocyte chemoattractant protein-1 (CCL2)
MEG-01	Human megakaryoblastic leukemia cell line
MKs	Megakaryocytes
MISEV 2023	Minimal Information for Studies of Extracellular Vesicles 2023 guidelines
MIP-1α	Macrophage inflammatory protein-1 alpha (CCL3)
MTOR	Mechanistic target of rapamycin
N_2	Nitrogen
NTA	Nanoparticle tracking analysis
nRBC-EVs	Extracellular vesicles derived from non-infected red blood cells
nRBCs	Non-infected red blood cells
NOTCH3	Neurogenic locus notch homolog protein 3

NOX1	NADPH oxidase 1
O_2	Oxygen
PBS	Phosphate-buffered saline
PDGFRB	Platelet-derived growth factor receptor beta
PKC	Protein kinase C
PMA	Phorbol 12-myristate 13-acetate
PLPs	Platelet-like particles
PPP	Platelet-poor plasma
PRP	Platelet-rich plasma
pRBC-EVs	Extracellular vesicles derived from *Plasmodium falciparum*–infected red blood cells
pRBCs	*Plasmodium falciparum*–infected red blood cells
P. falciparum	*Plasmodium falciparum*
qPCR	Quantitative polymerase chain reaction
RANTES	Regulated on Activation, Normal T Cell Expressed and Secreted (CCL5)
RPMI	Roswell Park Memorial Institute medium
RT-PCR	Reverse transcription polymerase chain reaction

Acknowledgements

This research was funded by the Thailand Science Research and Innovation Fund, Chulalongkorn University (HEA_FF_68_064_3700_001). Additional support was provided by the National Research Council of Thailand (NRCT) under the Research Grant for Joint Funding (NRCT5-RGJ63001-008). The authors would like to thank the Australian Red Cross Lifeblood for providing

de-identified human blood products used in this study and the University of Technology Sydney (UTS) for technical support and access to research facilities. The authors are also grateful to laboratory members and collaborators for valuable discussions and assistance throughout this work.

Author contributions

N.N. conceived and designed the study, performed formal analysis, and prepared the original draft of the manuscript. N.N. and A.P. performed data analysis and contributed to data interpretation. D.P. contributed to conceptualization and study design. V.C. supervised the project, provided visualization and conceptual input, and critically revised the manuscript. N.N. wrote the manuscript with input from all authors. All authors reviewed and approved the final version of the manuscript.

Funding

This study was supported by the Thailand Science Research and Innovation Fund, Chulalongkorn University (HEA_FF_68_064_3700_001), and the National Research Council of Thailand (NRCT) (NRCT5-RGJ63001-008). The funding agencies had no role in study design, data collection and analysis, decision to publish, or preparation of the manuscript.

Data availability

All data generated or analyzed during this study are included in this published article and its Additional file 1.

Declarations

Ethics approval and consent to participate

All experimental procedures were conducted in accordance with the principles of ICH-GCP guidelines. Ethical approval for this study was granted by the Chulalongkorn University Research Ethics Committee (COA No. 186/67), the University of Technology Sydney Human Research Ethics Committee (ETH20-5280), and the Australian Red Cross Lifeblood Ethics Committee (ETH24-9504). Human blood samples were obtained from anonymized donor units, and written informed consent was not required as per the approved institutional protocols.

Consent for publication

Not applicable.

Competing interests

The authors declare that they have no competing interests.

References

1. Organization WH. Malaria Fact Sheet. Geneva, Switzerland: World Health Organization. 2023.

2. Lacerda MV, Mourão MP, Coelho HC, Santos JB. Thrombocytopenia in malaria: who cares? Mem Inst Oswaldo Cruz. 2011;106 Suppl 1:52-63.

3. Bayleyegn B, Asrie F, Yalew A, Woldu B. Role of Platelet Indices as a Potential Marker for Malaria Severity. J Parasitol Res. 2021;2021:5531091.

4. O'Sullivan JM, O'Donnell JS. Platelets in malaria pathogenesis. Blood. 2018;132(12):1222-4.

5. Gupta NK, Bansal SB, Jain UC, Sahare K. Study of thrombocytopenia in patients of malaria. Trop Parasitol. 2013;3(1):58-61.

6. Machlus KR, Italiano JE, Jr. The incredible journey: From megakaryocyte development to platelet formation. J Cell Biol. 2013;201(6):785-96.

7. Kumar MA, Baba SK, Sadida HQ, Marzooqi SA, Jerobin J, Altemani FH, et al. Extracellular vesicles as tools and targets in therapy for diseases. Signal Transduction and Targeted Therapy. 2024;9(1):27.

8. Sampaio NG, Emery SJ, Garnham AL, Tan QY, Sisquella X, Pimentel MA, et al. Extracellular vesicles from early stage Plasmodium falciparum-infected red blood cells contain PfEMP1 and induce transcriptional changes in human monocytes. Cell Microbiol. 2018;20(5):e12822.

9. Kapur R, Semple JW. Megakaryocytes listen for their progeny's progeny during inflammation. J Thromb Haemost. 2021;19(3):604-6.

10. Vimonpatranon S, Roytrakul S, Phaonakrop N, Lekmanee K, Atipimonpat A, Srimark N, et al. Extracellular Vesicles Derived from Early and Late Stage Plasmodium falciparum-Infected Red Blood Cells Contain Invasion-Associated Proteins. J Clin Med. 2022;11(14).

11. Dey S, Mohapatra S, Khokhar M, Hassan S, Pandey RK. Extracellular Vesicles in Malaria: Shedding Light on Pathogenic Depths. ACS Infect Dis. 2024;10(3):827-44.

12. Mantel P-Y, Hoang Anh N, Goldowitz I, Potashnikova D, Hamza B, Vorobjev I, et al. Malaria-Infected Erythrocyte-Derived Microvesicles Mediate Cellular Communication within the Parasite Population and with the Host Immune System. Cell Host & Microbe. 2013;13(5):521-34.

13. Borgheti-Cardoso LN, Kooijmans SAA, Chamorro LG, Biosca A, Lantero E, Ramírez M, et al. Extracellular vesicles derived from Plasmodium-infected and non-infected red blood cells as targeted drug delivery vehicles. International Journal of Pharmaceutics. 2020;587:119627.

14. Mantel P-Y, Hjelmqvist D, Walch M, Kharoubi-Hess S, Nilsson S, Ravel D, et al. Infected erythrocyte-derived extracellular vesicles alter vascular function via regulatory Ago2-miRNA complexes in malaria. Nature Communications. 2016;7(1):12727.

15. Regev-Rudzki N, Wilson DW, Carvalho TG, Sisquella X, Coleman BM, Rug M, et al. Cell-cell communication between malaria-infected red blood cells via exosome-like vesicles. Cell. 2013;153(5):1120-33.

16. Sisquella X, Ofir-Birin Y, Pimentel MA, Cheng L, Abou Karam P, Sampaio NG, et al. Malaria parasite DNA-harbouring vesicles activate cytosolic immune sensors. Nature Communications. 2017;8(1):1985.

17. Babatunde KA, Yesodha Subramanian B, Ahouidi AD, Martinez Murillo P, Walch M, Mantel PY. Role of Extracellular Vesicles in Cellular Cross Talk in Malaria. Front Immunol. 2020;11:22.

18. Pankoui Mfonkeu JB, Gouado I, Fotso Kuaté H, Zambou O, Amvam Zollo PH, Grau GE, et al. Elevated cell-specific microparticles are a biological marker for cerebral dysfunctions in human severe malaria. PLoS One. 2010;5(10):e13415.

19. Nantakomol D, Dondorp AM, Krudsood S, Udomsangpetch R, Pattanapanyasat K, Combes V, et al. Circulating red cell-derived microparticles in human malaria. J Infect Dis. 2011;203(5):700-6.

20. Coltel N, Combes V, Hunt NH, Grau GE. Cerebral malaria -- a neurovascular pathology with many riddles still to be solved. Curr Neurovasc Res. 2004;1(2):91-110.

21. Noetzli LJ, French SL, Machlus KR. New Insights Into the Differentiation of Megakaryocytes From Hematopoietic Progenitors. Arteriosclerosis, Thrombosis, and Vascular Biology. 2019;39(7):1288-300.

22. Pang L, Weiss MJ, Poncz M. Megakaryocyte biology and related disorders. J Clin Invest. 2005;115(12):3332-8.

23. Mercher T, Cornejo MG, Sears C, Kindler T, Moore SA, Maillard I, et al. Notch signaling specifies megakaryocyte development from hematopoietic stem cells. Cell Stem Cell. 2008;3(3):314-26.

24. Jie Yu Y, Godfrey Chi Fung C, Liang Q, Qizhou L, Fan Yi M, Xue Qun L, et al. Platelet-derived growth factor enhances platelet recovery in a murine model of radiation-induced thrombocytopenia and reduces apoptosis in megakaryocytes via its receptors and the PI3-k/Akt pathway. Haematologica. 2010;95(10):1745-53.

25. McMorran BJ, Marshall VM, de Graaf C, Drysdale KE, Shabbar M, Smyth GK, et al. Platelets kill intraerythrocytic malarial parasites and mediate survival to infection. Science. 2009;323(5915):797-800.

26. van der Heyde HC, Nolan J, Combes V, Gramaglia I, Grau GE. A unified hypothesis for the genesis of cerebral malaria: sequestration, inflammation and hemostasis leading to microcirculatory dysfunction. Trends Parasitol. 2006;22(11):503-8.

27. Grau GE, Craig AG. Cerebral malaria pathogenesis: revisiting parasite and host contributions. Future Microbiol. 2012;7(2):291-302.

28. Ogura M, Morishima Y, Ohno R, Kato Y, Hirabayashi N, Nagura H, et al. Establishment of a novel human megakaryoblastic leukemia cell line, MEG-01, with positive Philadelphia chromosome. Blood. 1985;66(6):1384-92.

29. Mata-Cantero L, Lafuente MJ, Sanz L, Rodriguez MS. Magnetic isolation of Plasmodium falciparum schizonts iRBCs to generate a high parasitaemia and synchronized in vitro culture. Malaria Journal. 2014;13(1):112.

30. White NJ. Anaemia and malaria. Malaria Journal. 2018;17(1):371.

31. Aguilar R, Magallon-Tejada A, Achtman AH, Moraleda C, Joice R, Cisteró P, et al. Molecular evidence for the localization of Plasmodium falciparum immature gametocytes in bone marrow. Blood. 2014;123(7):959-66.

32. Joice R, Nilsson SK, Montgomery J, Dankwa S, Egan E, Morahan B, et al. Plasmodium falciparum transmission stages accumulate in the human bone marrow. Sci Transl Med. 2014;6(244):244re5.

33. Banerjee A, Tripathi A, Duggal S, Banerjee A, Vrati S. Dengue virus infection impedes megakaryopoiesis in MEG-01 cells where the virus envelope protein interacts with the transcription factor TAL-1. Scientific Reports. 2020;10(1):19587.

34. Persson KM, Kneller PV, Livingston MW, Bush LM, Deans TL. High-Throughput Production of Platelet-Like Particles. Methods Mol Biol. 2021;2258:273-83.

35. Murray NR, Baumgardner GP, Burns DJ, Fields AP. Protein kinase C isotypes in human erythroleukemia (K562) cell proliferation and differentiation. Evidence that beta II protein kinase C is required for proliferation. J Biol Chem. 1993;268(21):15847-53.

36. Lee DY, Lee SY, Yun SH, Jeong JW, Kim JH, Kim HW, et al. Review of the Current Research on Fetal Bovine Serum and the Development of Cultured Meat. Food Sci Anim Resour. 2022;42(5):775-99.

37. Huang Y, Fu Z, Dong W, Zhang Z, Mu J, Zhang J. Serum starvation-induces down-regulation of Bcl-2/Bax confers apoptosis in tongue coating-related cells in vitro. Mol Med Rep. 2018;17(4):5057-64.

38. van Besien K, Loberiza FR, Jr, Bajorunaite R, Armitage JO, Bashey A, Burns LJ, et al. Comparison of autologous and allogeneic hematopoietic stem cell transplantation for follicular lymphoma. Blood. 2003;102(10):3521-9.

39. You T, Wang Q, Zhu L. Role of autophagy in megakaryocyte differentiation and platelet formation. Int J Physiol Pathophysiol Pharmacol. 2016;8(1):28-34.

40. Fujimoto TT, Kohata S, Suzuki H, Miyazaki H, Fujimura K. Production of functional platelets by differentiated embryonic stem (ES) cells in vitro. Blood. 2003;102(12):4044-51.

41. Obaldia N, 3rd, Meibalan E, Sa JM, Ma S, Clark MA, Mejia P, et al. Bone Marrow Is a Major Parasite Reservoir in Plasmodium vivax Infection. mBio. 2018;9(3).

42. Gama-Norton L, Ferrando E, Ruiz-Herguido C, Liu Z, Guiu J, Islam ABMMK, et al. Notch signal strength controls cell fate in the haemogenic endothelium. Nature Communications. 2015;6(1):8510.

43. Raposo G, Stoorvogel W. Extracellular vesicles: exosomes, microvesicles, and friends. J Cell Biol. 2013;200(4):373-83.

44. Colombo M, Raposo G, Théry C. Biogenesis, secretion, and intercellular interactions of exosomes and other extracellular vesicles. Annu Rev Cell Dev Biol. 2014;30:255-89.

45. Willekens FLA, Werre JM, Groenen-Döpp YAM, Roerdinkholder-Stoelwinder B, De Pauw B, Bosman GJCGM. Erythrocyte vesiculation: a self-protective mechanism? British Journal of Haematology. 2008;141(4):549-56.

46. Bosman G. Survival of red blood cells after transfusion: processes and consequences. Frontiers in Physiology. 2013;Volume 4 - 2013.

Figures legend

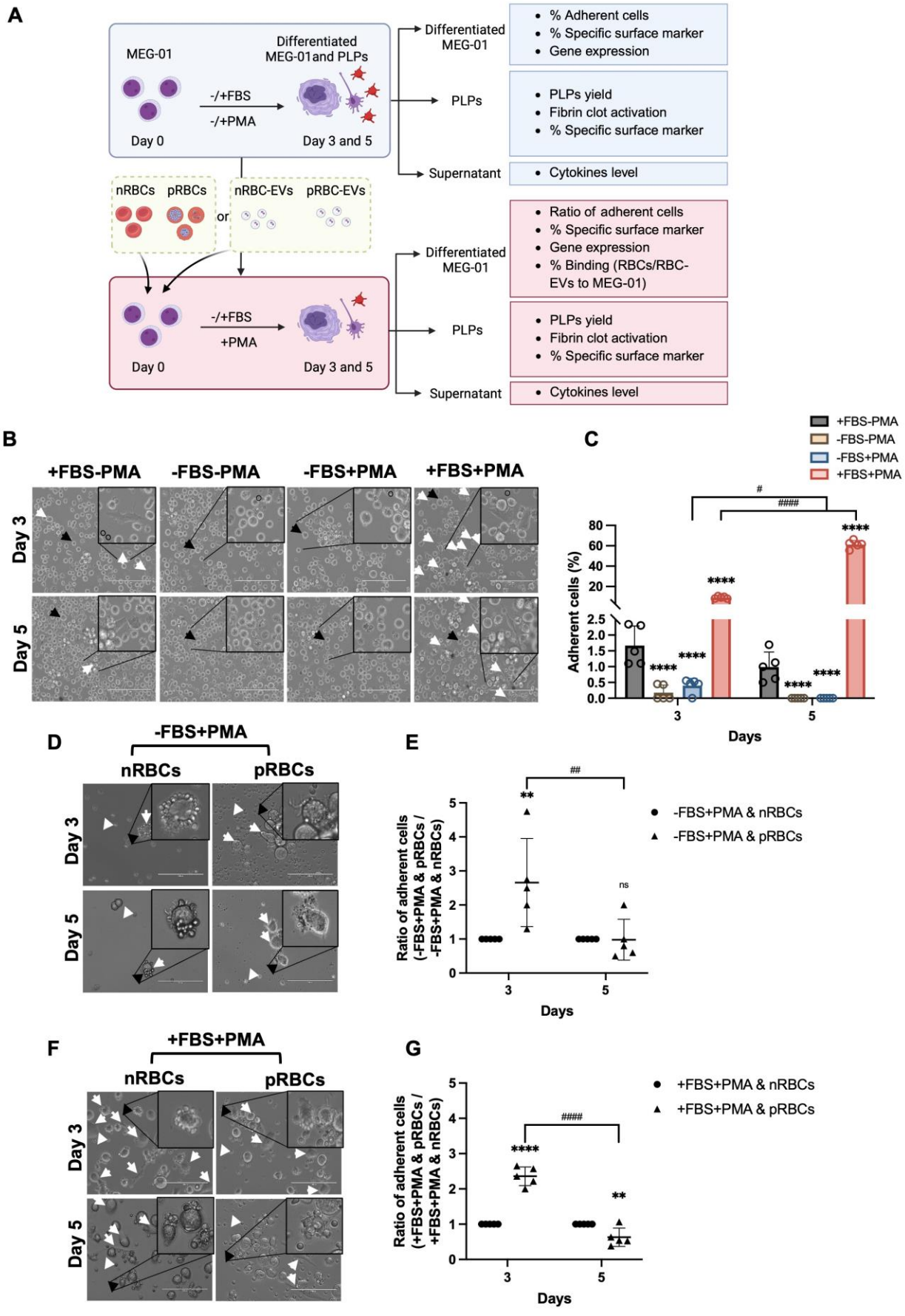
A
MEG-01
Differentiated MEG-01and PLPs
-/+FBS
-/+PMA
Day 0
Day 3 and 5
Differentiated MEG-01
PLPs
Supernatant
% Adherent cells
% Specific surface marker
Gene expression
PLPs yield
Fibrin clot activation
% Specific surface marker
Cytokines level
nRBCs
pRBCs
nRBC-EVs
pRBC-EVs
or
Ratio of adherent cells
% Specific surface marker
Gene expression
% Binding (RBCs/RBC-EVs to MEG-01)
+PMA
B
+FBS-PMA
-FBS-PMA
-FBS+PMA
+FBS+PMA
Day 3
Day 5
C
Adherent cells (%)
Days
D
E
Ratio of adherent cells (-FBS+PMA & pRBCs / -FBS+PMA & nRBCs)
-FBS+PMA & nRBCs
-FBS+PMA & pRBCs
F
G
Ratio of adherent cells (+FBS+PMA & pRBCs / +FBS+PMA & nRBCs)
+FBS+PMA & nRBCs
+FBS+PMA & pRBCs

Fig. 1 Adherence of MEG-01 cells under different culture conditions and binding interactions between MEG-01 cells and RBCs. (a) Schematic diagram representing PLP production from MEG-01 and co-culture with nRBCs, pRBCs, nRBC-EVs, or pRBC-EVs, followed by the collection of constituents for subsequent testing. **(b, d, f)** Phase-contrast images of MEG-01 cells on days 3 and 5 under various culture conditions. **(b)** MEG-01 cells were cultured with or without FBS and PMA. Floating cells are marked by black arrows, adherent cells by white arrows, and PLPs by circles. Scale bar: 100 μm (20×). **(d, f)** Co-culture of MEG-01 cells with nRBCs or pRBCs under −FBS/+PMA and +FBS/+PMA conditions, respectively. White triangles indicate RBCs. Insets highlight direct binding interactions between MEG-01 cells and RBCs. Scale bars: 200 μm (40×). **(c, e, g)** Quantification of adherent MEG-01 cells. **(c)** Percentage of adherent cells on days 3 and 5. **(e, g)** Ratios of adherent cells in co-cultures with nRBCs or pRBCs under −FBS/+PMA or +FBS/+PMA conditions, respectively. Statistical significance: $^{**}p < 0.01$, $^{****}p < 0.001$ between conditions; $\#p < 0.05$, $\#\#p < 0.01$, $\#\#\#\#p < 0.001$ within the same condition across different days; ns = non-significant.

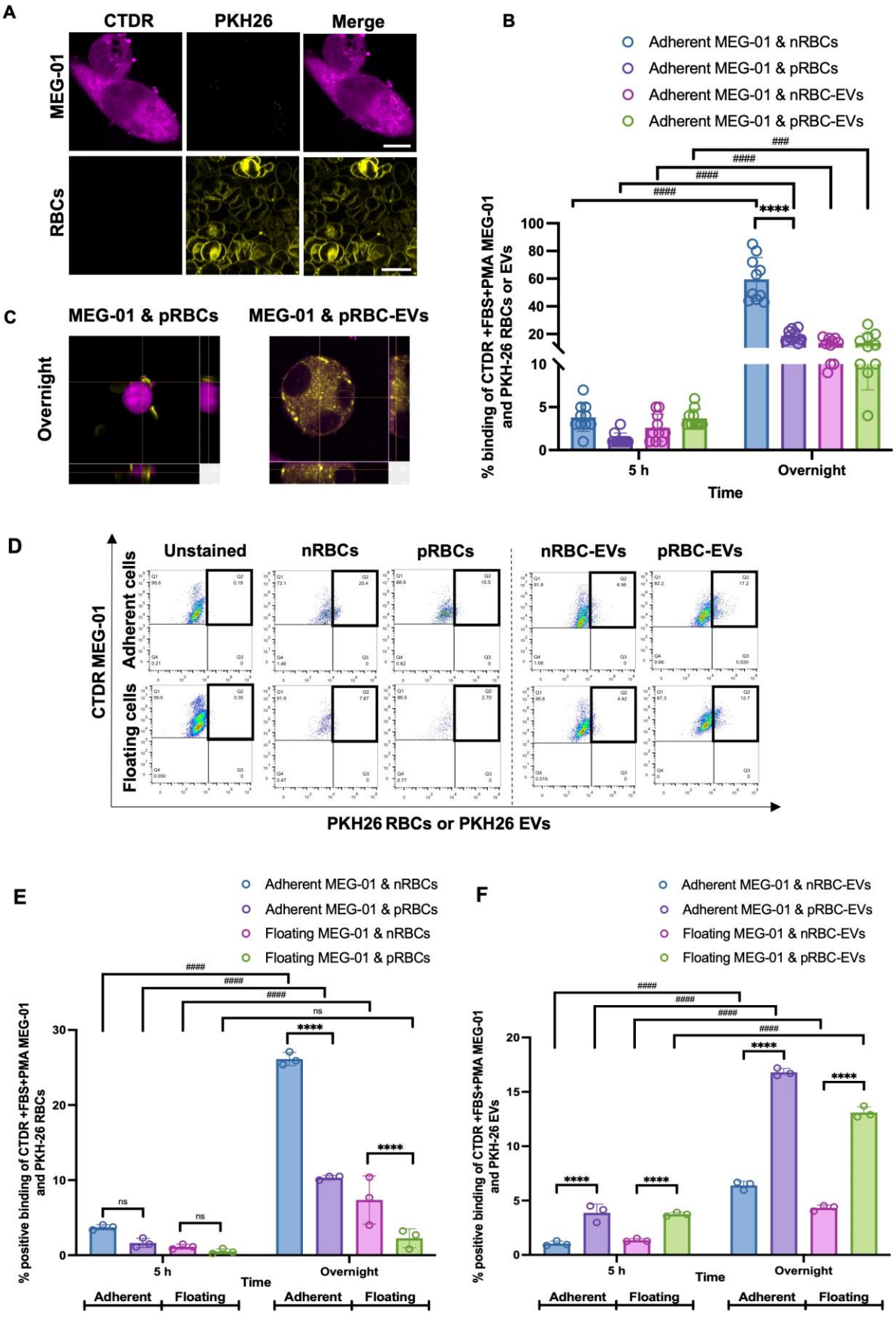
A
CTDR
PKH26
Merge
MEG-01
RBCs
B
Adherent MEG-01 & nRBCs
Adherent MEG-01 & pRBCs
Adherent MEG-01 & nRBC-EVs
Adherent MEG-01 & pRBC-EVs
% binding of CTDR +FBS+PMA MEG-01 and PKH-26 RBCs or EVs
5 h
Overnight
Time
C
MEG-01 & pRBCs
MEG-01 & pRBC-EVs
Overnight
D
Unstained
nRBCs
pRBCs
nRBC-EVs
pRBC-EVs
Adherent cells
Floating cells
CTDR MEG-01
PKH26 RBCs or PKH26 EVs
E
Adherent MEG-01 & nRBCs
Adherent MEG-01 & pRBCs
Floating MEG-01 & nRBCs
Floating MEG-01 & pRBCs
% positive binding of CTDR +FBS+PMA MEG-01 and PKH-26 RBCs
5 h
Overnight
Time
Adherent
Floating
F
Adherent MEG-01 & nRBC-EVs
Adherent MEG-01 & pRBC-EVs
Floating MEG-01 & nRBC-EVs
Floating MEG-01 & pRBC-EVs
% positive binding of CTDR +FBS+PMA MEG-01 and PKH-26 EVs

Fig. 2 Binding of RBCs and RBC-EVs to MEG-01 cells after 5 h and overnight incubation. **(a)** Confocal images showing MEG-01 cells (cytoplasm stained with CTDR; magenta) and RBCs (membrane stained with PKH26; yellow). Scale bar: 10 μm (100×). **(b)** Quantification of binding between CTDR-labeled MEG-01 cells and PKH26-labeled RBCs or RBC-EVs using ImageJ. Binding events were counted in 10 randomly selected fields or normalized per 1,000 adherent MEG-01 cells at 5 h and overnight. **(c)** Z-stack confocal images showing binding interactions between MEG-01 cells and either RBCs or RBC-EVs after overnight co-culture. **(d)** Flow cytometry gating of double-positive nRBCs, pRBCs, nRBC-EVs, and pRBC-EVs bound to adherent or floating MEG-01 cells. **(e, f)** Bar graphs showing the percentage of CTDR-positive adherent and floating MEG-01 cells (+FBS/+PMA condition) after co-incubation with PKH26-labeled nRBCs/pRBCs **(e)** or nRBC-EVs/pRBC-EVs **(f)** for 5 h and overnight; n = 3. Statistical significance: ****$p < 0.001$ between conditions; ###$p < 0.005$, ####$p < 0.001$ between time points within the same condition; ns = not significant.

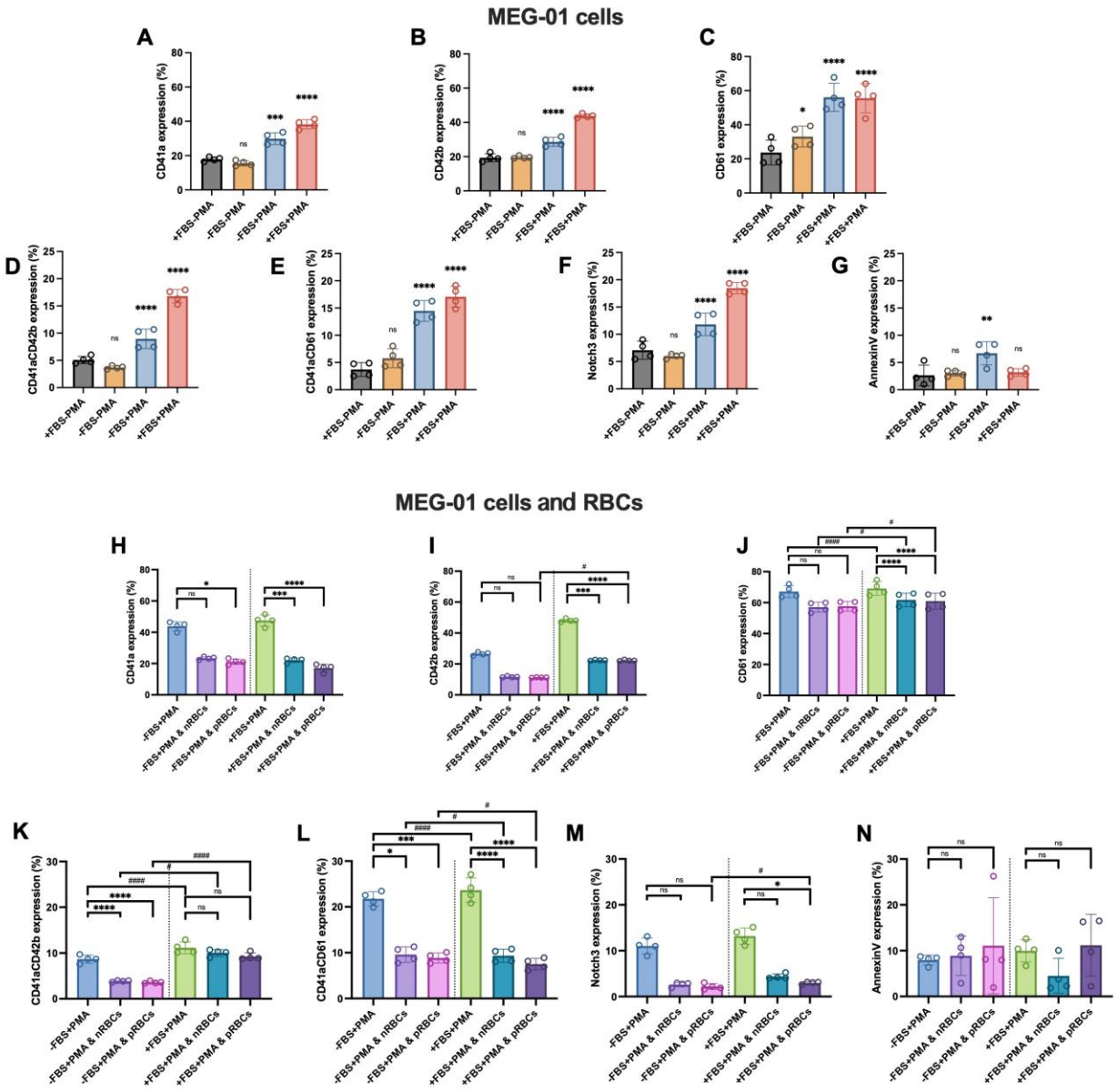

Fig. 3 Expression of surface markers on MEG-01 cells under different culture conditions and during co-culture with RBCs. Flow cytometry was used to assess surface marker expression on MEG-01 cells cultured under various conditions for 5 days. **(a–g)** Bar graphs showing the expression of CD41a, CD42b, CD61, $CD41a^{+}CD42b^{+}$, $CD41a^{+}CD61^{+}$ double-positive cells, Notch3, and Annexin V in MEG-01 cells cultured with or without FBS and PMA; n = 4. **(h–n)** Expression of the same markers in MEG-01 cells co-cultured with nRBCs or pRBCs under

−FBS/+PMA and +FBS/+PMA conditions. All marker levels are expressed as the percentage of positive MEG-01 cells; n = 4. Statistical significance: *$p < 0.05$, **$p < 0.01$, ***$p < 0.005$, ****$p < 0.001$ between conditions; #$p < 0.05$, ####$p < 0.001$ between condition within the same treatments; ns = not significant.

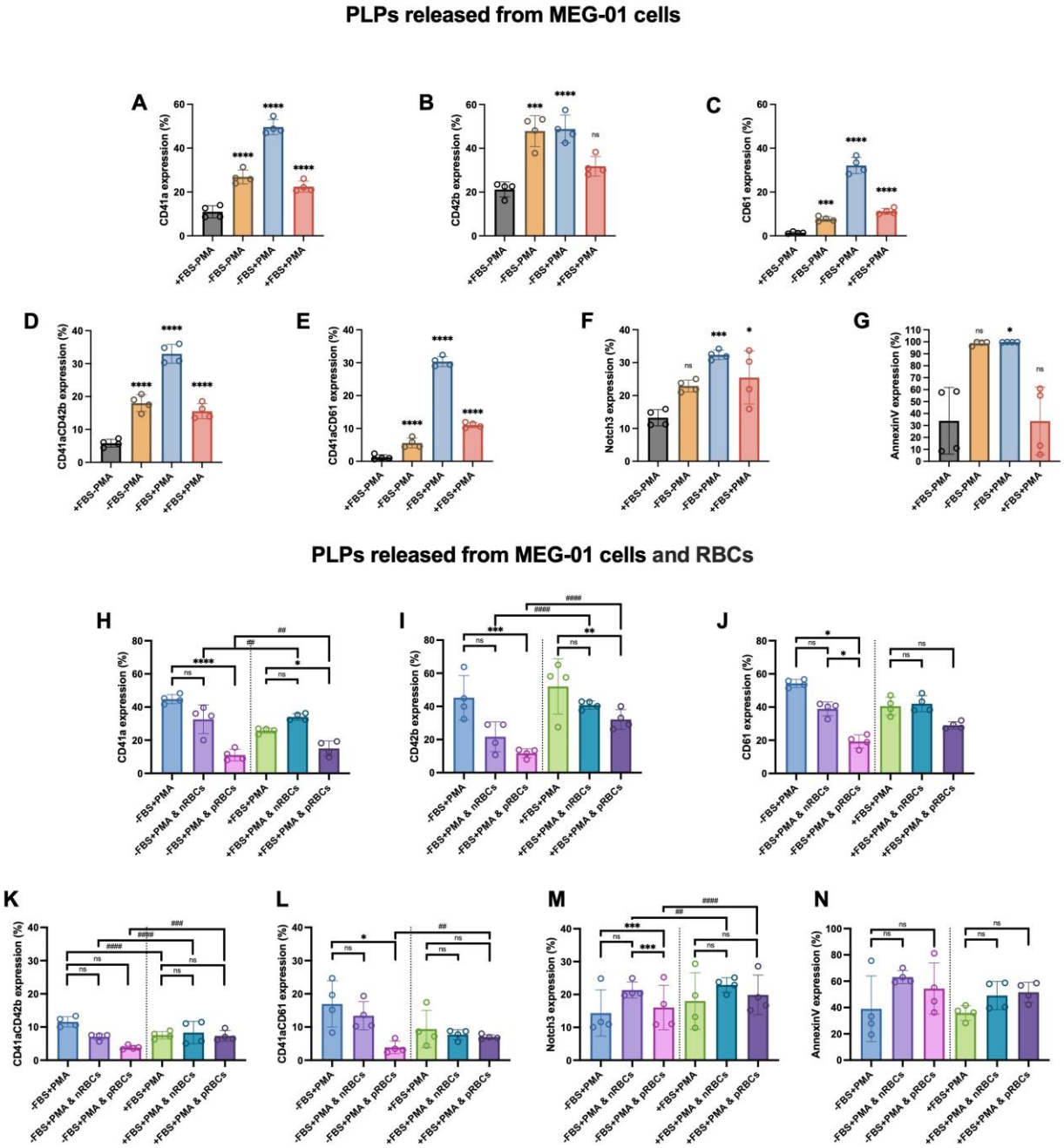

Fig. 4 Expression of surface markers on PLPs derived from MEG-01 cells under different

culture conditions and during co-culture with RBCs. Flow cytometry was used to assess the expression of surface markers on PLPs collected from MEG-01 cultures for 5 days. **(a–g)** Bar graphs showing the expression of CD41a, CD42b, CD61, $CD41a^{+}CD42b^{+}$, $CD41a^{+}CD61^{+}$ double-positive cells, Notch3, and Annexin V in PLPs generated with or without FBS and PMA stimulation; n = 4. **(h–n)** Expression of the same markers in PLPs derived from MEG-01 cells co-cultured with nRBCs or pRBCs under −FBS/+PMA and +FBS/+PMA conditions; n = 4. All values represent the percentage of marker-positive PLPs. Statistical significance: $*p < 0.05$, $**p < 0.01$, $***p < 0.005$, $****p < 0.001$ between conditions; $\#\#p < 0.01$, $\#\#\#p < 0.005$, $\#\#\#\#p < 0.001$ between condition within the same treatments; ns = not significant.

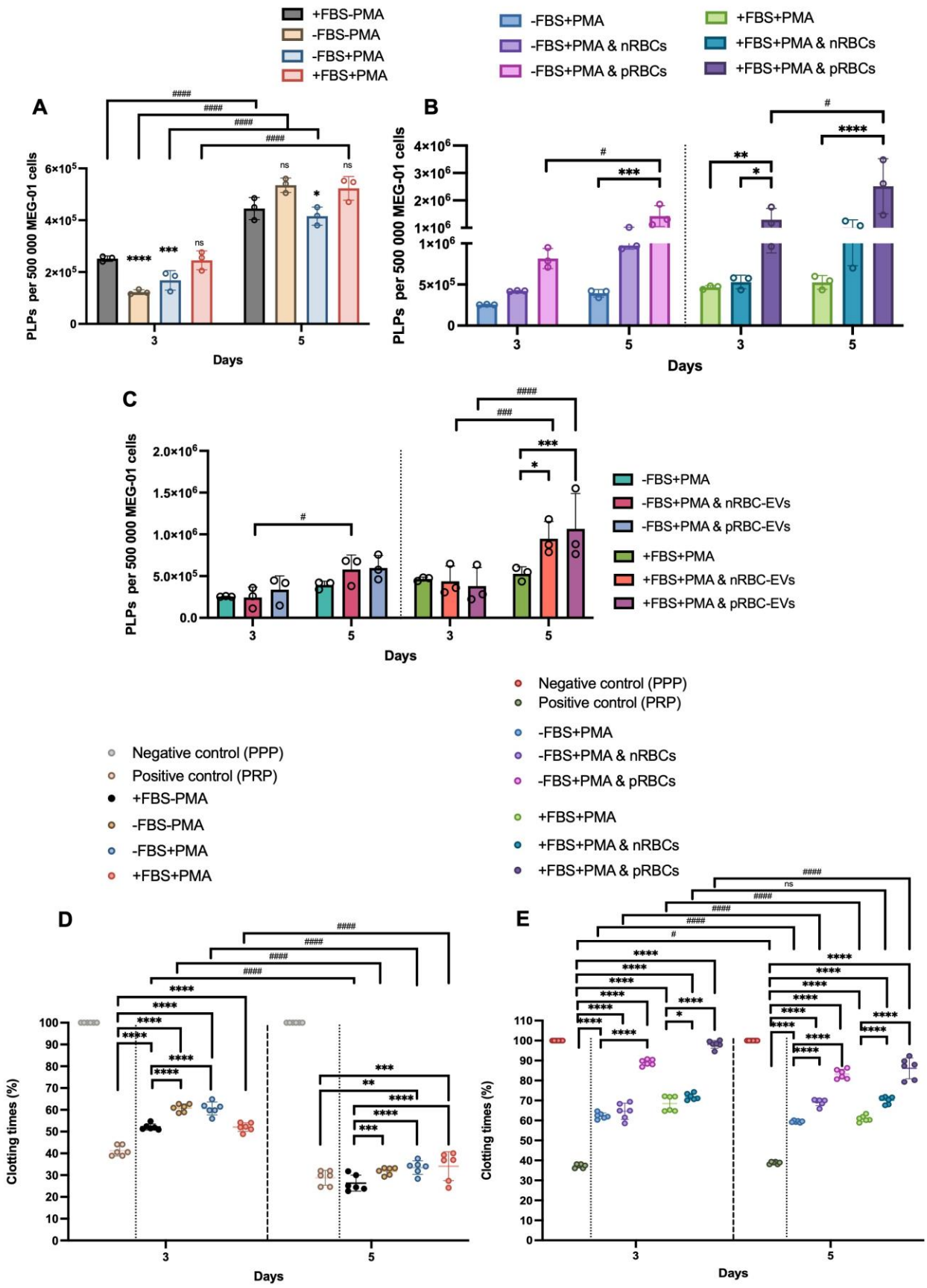
+FBS-PMA
-FBS-PMA
-FBS+PMA
+FBS+PMA
A
PLPs per 500 000 MEG-01 cells
Days
-FBS+PMA
-FBS+PMA & nRBCs
-FBS+PMA & pRBCs
+FBS+PMA
+FBS+PMA & nRBCs
+FBS+PMA & pRBCs
B
C
-FBS+PMA & nRBC-EVs
-FBS+PMA & pRBC-EVs
+FBS+PMA & nRBC-EVs
+FBS+PMA & pRBC-EVs
Negative control (PPP)
Positive control (PRP)
D
E
Clotting times (%)

Fig. 5 Production and functional activity of PLPs derived from MEG-01 cells under different culture conditions and during co-culture with RBCs or RBC-EVs. PLPs were collected from culture supernatants by centrifugation at 500 × g for 10 min and counted using a Malassez chamber. **(a)** Bar graph showing the number of PLPs per 500,000 MEG-01 cells on days 3 and 5 under different culture conditions; n = 3. **(b)** PLP counts from MEG-01 cells co-cultured with nRBCs or pRBCs with or without FBS and PMA; n = 3. **(c)** Similar analysis for co-cultures with nRBC-EVs or pRBC-EVs; n = 3. **(d)** Clotting activity of PLPs expressed as percentage of clotting time relative to platelet-poor plasma (PPP; negative control) and platelet-rich plasma (PRP; positive control) on days 3 and 5; n = 6. **(e)** Clotting time of PLPs produced with nRBCs or pRBCs was compared between −FBS/+PMA and +FBS/+PMA conditions; n = 6. Statistical significance: $*p < 0.05$, $**p < 0.01$, $***p < 0.005$, $****p < 0.001$ between conditions; $\#p < 0.05$, $\#\#\#p < 0.005$, $\#\#\#\#p < 0.001$ within the same condition; ns = not significant.

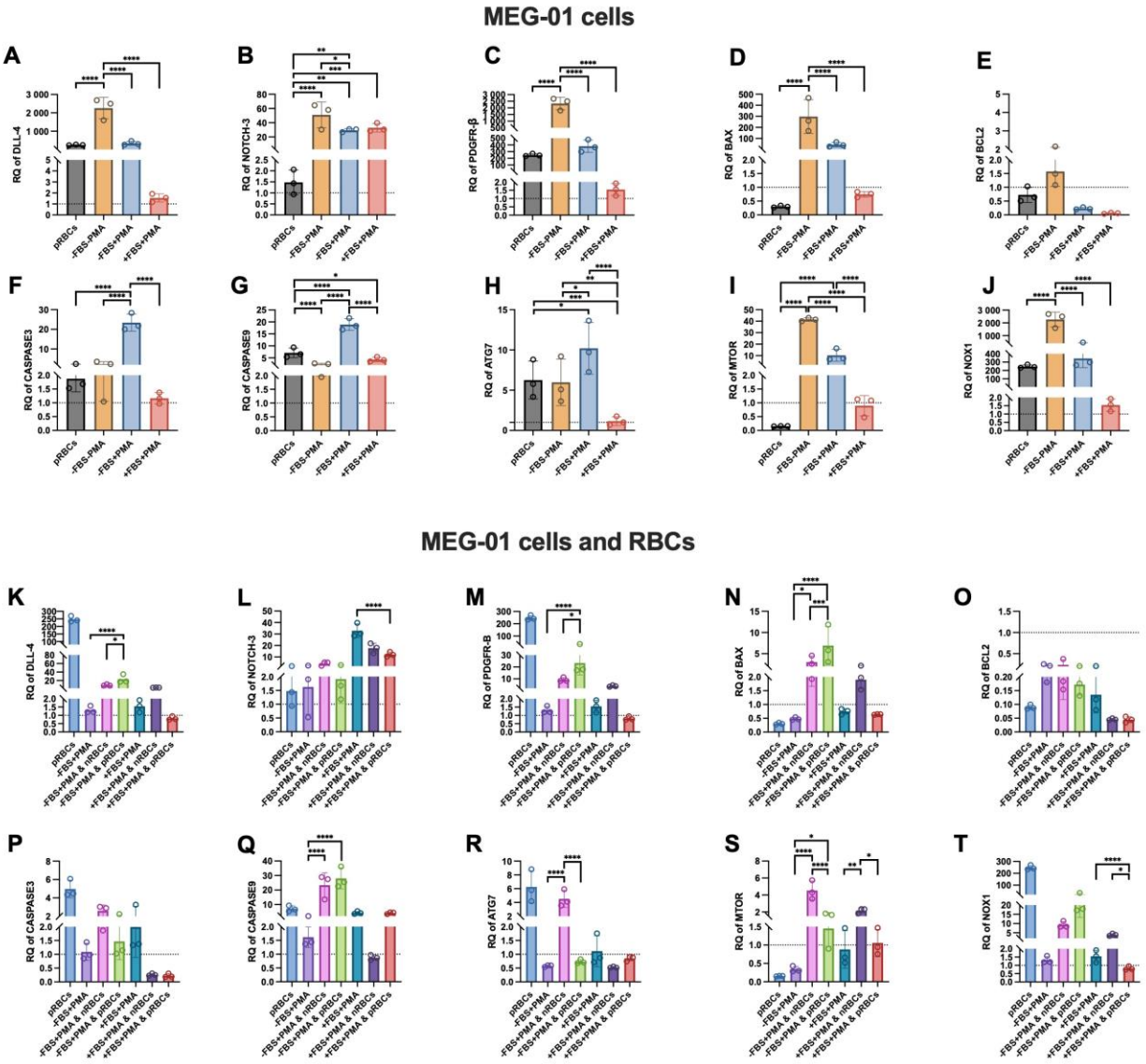

Fig. 6 Gene expression in MEG-01 cells under different culture conditions and during co-culture with RBCs. Relative gene expression in MEG-01 cells was analyzed on day 5 under various conditions, with or without FBS and PMA stimulation, and during co-culture with RBCs. **(a–j)** Bar graphs showing expression of key genes in MEG-01 cells cultured under four conditions: DLL4 **(a)**, which impairs terminal megakaryocytic differentiation; NOTCH3 **(b)**, a proliferation regulator; PDGFRB **(c)**, associated with platelet function; BAX **(d)** and BCL2 **(e)**, apoptosis regulators; CASPASE3 **(f)** and CASPASE9 **(g)**, pro-apoptotic markers; ATG7 **(h)**, MTOR **(i)**, and

NOX1 **(j)**, related to autophagy and oxidative stress. **(k–t)** Expression of the same genes in MEG-01 cells co-cultured with nRBCs or pRBCs under −FBS/+PMA and +FBS/+PMA conditions; n = 3. Gene expression was quantified by RT-PCR and normalized to glyceraldehyde-3-phosphate dehydrogenase (GAPDH). Data are expressed as relative fold changes, with +FBS/−PMA set to 1. Statistical significance: *$p < 0.05$, **$p < 0.01$, ***$p < 0.005$, ****$p < 0.001$ between conditions.

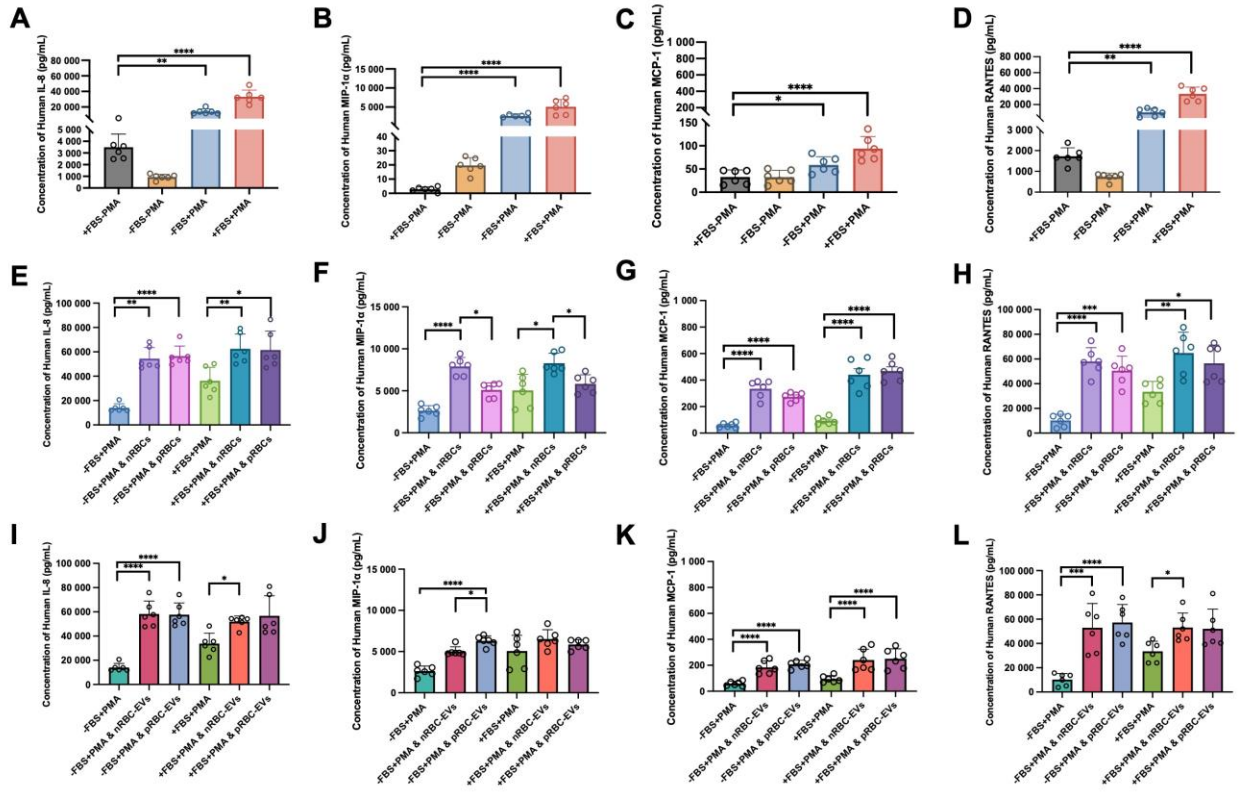

Fig. 7 Cytokine profiling in MEG-01 cultures under different conditions and during co-culture with RBCs or RBC-EVs. Cytokine concentrations were measured in MEG-01 culture supernatants collected on day 3 under various conditions. **(a–d)** Bar graphs showing concentrations of human IL-8 **(a)**, MIP-1α **(b)**, RANTES **(c)**, and MCP-1 **(d)** under different culture conditions. **(e–h)** Cytokine levels in cultures co-incubated with nRBCs or pRBCs in the presence or absence of FBS and PMA. **(i–l)** Cytokine levels in cultures co-incubated with nRBC-EVs or pRBC-EVs

under the same conditions; n = 6. All values represent cytokine concentrations (pg/ml). Statistical significance: *$p < 0.05$, **$p < 0.01$, ***$p < 0.005$, ****$p < 0.001$ between conditions.

Supplementary Information

Fig. S1 Characterization of RBC-EVs. (a) Representative flow cytometry plots showing PKH26-positive events from isolated nRBC-EVs and pRBC-EVs (1:3,200 EVs: PBS); PBS served as a blank control. **(b)** Linear correlations of PKH26-positive EV count for nRBC-EVs (R^2 = 0.9976) and pRBC-EVs (R^2 = 0.9982); n = 3. **(c)** NTA showing particle concentration, size distribution, and representative images of nRBC-EVs and pRBC-EVs (1:2,000 EVs: PBS); n = 3. **(d)** Scatter plot of particle concentrations for nRBC-EVs and pRBC-EVs; n = 3. Each dot represents one sample.

Fig. S2 Adherence of MEG-01 cells co-cultured with RBC-EVs under different culture conditions. (a) Phase-contrast images of MEG-01 cells co-cultured with EVs derived from nRBCs or pRBCs on days 3 and 5 under –FBS/+PMA and +FBS/+PMA conditions, respectively. Adherent cells are indicated by white arrows. Scale bar: 200 μm, (40×). **(b, c)** Quantification of adherent MEG-01 cells co-cultured with nRBC-EVs or pRBC-EVs under –FBS/+PMA and +FBS/+PMA conditions, respectively; n = 6. Statistical significance: #$p < 0.05$ indicates comparisons within the same condition across different days; ns = non-significant.

Fig. S3 Binding of RBCs or RBC-EVs to MEG-01 cells at 5 h and overnight, observed by fluorescence microscopy. Confocal microscopy images show the binding interactions between MEG-01 cells and RBCs or RBC-EVs after 5 h and overnight co-culture. The cytoplasm of MEG-01 cells was stained with CTDR (magenta), and RBCs were stained with PKH26 (yellow). Nuclei were counterstained with DAPI. Scale bar: 10 μm, (100×). **(a)** Binding between MEG-01 cells and

either nRBCs or pRBCs. **(b)** Binding between MEG-01 cells and either nRBC-EVs or pRBC-EVs. **(c)** Z-stack images of MEG-01–RBC interactions. **(d)** Z-stack images of MEG-01–RBC-EV interactions after 5-hour and overnight co-culture.

Fig. S4 Binding of RBCs or RBC-EVs to adherent and floating MEG-01 cells at 5 h and overnight, observed by fluorescence microscopy. Confocal microscopy images showing binding interactions between adherent or floating MEG-01 cells and RBCs or RBC-EVs after 5-hour and overnight co-culture. MEG-01 cytoplasm was stained with CTDR (magenta), RBCs with PKH26 (yellow), and nuclei with DAPI. **(a)** Binding between adherent MEG-01 cells and either nRBCs or pRBCs. **(b)** Binding between adherent MEG-01 cells and either nRBC-EVs or pRBC-EVs. Scale bar: 10 μm, (20×). **(c)** Binding between floating MEG-01 cells and either nRBCs or pRBCs. **(d)** Binding between floating MEG-01 cells and either nRBC-EVs or pRBC-EVs. Scale bar: 20 μm, (10×).

Fig. S5 Binding of RBCs or RBC-EVs to MEG-01 cells at 5 h and overnight, analyzed by flow cytometry. Flow cytometry gating of double-positive nRBCs, pRBCs, nRBC-EVs, and pRBC-EVs bound to adherent or floating MEG-01 cells after 5-hour and overnight incubation. CTDR; Cell Tracker Deep Red Dye.

Fig. S6 Flow cytometry gating and histograms of specific surface markers on MEG-01 cells under different culture conditions, including co-culture with RBCs or RBC-EVs. (a) Gating strategy used for identifying MEG-01 cells and analyzing surface marker expression ($CD41a^+$, $CD42b^+$, $CD61^+$, $Notch3^+$, Annexin V^+). **(b)** Overlay histograms showing marker expression in MEG-01 cells cultured with or without FBS/PMA on days 3 and 5. **(c–d)** Gating strategy and representative histograms for MEG-01 cells co-cultured with nRBCs or pRBCs under –FBS/+PMA and +FBS/+PMA conditions. **(e–f)** Gating strategy and histograms for MEG-01 cells

co-cultured with nRBC-EVs or pRBC-EVs. All histograms include comparisons with unstained controls.

Fig. S7 Changes in specific surface markers on MEG-01 cells under various culture conditions, including co-culture with RBCs or RBC-EVs, on days 3 and 5. Flow cytometry analysis of marker expression on MEG-01 cells cultured under different conditions. **(a–g)** Expression of CD41a, CD42b, CD61, $CD41a^+CD42b^+$, $CD41a^+CD61^+$, Notch3, and Annexin V under control conditions. **(h–n)** Same markers for cells co-cultured with nRBCs or pRBCs under –FBS/+PMA and +FBS/+PMA conditions. **(o–u)** Expression of these markers in cells co-cultured with nRBC-EVs or pRBC-EVs. Data are expressed as the percentage of positive MEG-01 cells. Statistical significance: $*p < 0.05$, $**p < 0.01$, $***p < 0.005$, $****p < 0.001$; $\#p < 0.05$, $\#\#p < 0.01$, $\#\#\#p < 0.005$, $\#\#\#\#p < 0.001$ (within-condition comparisons); ns = non-significant.

Fig. S8 Flow cytometry gating and histograms of specific surface markers on PLPs released from MEG-01 cells under various culture conditions, including co-culture with RBCs or RBC-EVs. (a) Gating strategy for identifying PLPs and assessing surface marker expression ($CD41a^+$, $CD42b^+$, $CD61^+$, $Notch3^+$, Annexin V^+). **(b)** Overlay histograms showing marker expression in PLPs cultured with or without FBS/PMA on days 3 and 5. **(c–d)** Gating strategy and histograms for PLPs from MEG-01 cells co-cultured with nRBCs or pRBCs. **(e–f)** Gating strategy and histograms for PLPs from MEG-01 cells co-cultured with nRBC-EVs or pRBC-EVs. Overlay histograms represent expression at both time points under the respective conditions.

Fig. S9 Changes in specific surface markers on PLPs released from MEG-01 cells under various culture conditions, including co-culture with RBCs or RBC-EVs, on days 3 and 5. Flow cytometry analysis of surface marker expression in PLPs derived from MEG-01 cells. **(a–g)** CD41a, CD42b, CD61, $CD41a^+CD42b^+$, $CD41a^+CD61^+$, Notch3, and Annexin V expression under

control conditions. **(h–n)** Same markers for PLPs from MEG-01 cells co-cultured with nRBCs or pRBCs. **(o–u)** Expression of these markers in PLPs from MEG-01 cells co-cultured with nRBC-EVs or pRBC-EVs. All data are shown as the percentage of positive PLPs. Statistical significance: $*p < 0.05$, $**p < 0.01$, $***p < 0.005$, $****p < 0.001$; $\#p < 0.05$, $\#\#p < 0.01$, $\#\#\#p < 0.005$, $\#\#\#\#p < 0.001$ (within-condition comparisons); ns = non-significant.

Fig. S10 Gene expression of MEG-01 cells under various culture conditions, including co-culture with RBCs. Relative mRNA expression levels in MEG-01 cells were analyzed under different conditions, with or without FBS and PMA stimulation on day 3. **(a–j)** Expression of DLL4, NOTCH3, PDGFRB, BAX, BCL2, CASPASE3, CASPASE9, ATG7, MTOR, and NOX1. **(k–t)** Corresponding gene expression profiles in MEG-01 cells co-cultured with RBCs. Gene expression was normalized to GAPDH and expressed relative to +FBS/–PMA condition (set as 1). Statistical significance: $*p < 0.05$, $**p < 0.01$, $***p < 0.005$, $****p < 0.001$.

Fig. S11 Gene expression of MEG-01 cells under various culture conditions, including co-culture with RBC-EVs. Relative mRNA expression levels were analyzed under different conditions with or without FBS and PMA stimulation on days 3 and 5. **(a–j)** Expression of DLL4, NOTCH3, PDGFRB, BAX, BCL2, CASPASE3, CASPASE9, ATG7, MTOR, and NOX1 after co-culture with RBC-EVs. Gene expression was normalized to GAPDH and expressed relative to +FBS/–PMA condition (set as 1). Statistical significance: $*p < 0.05$, $**p < 0.01$, $***p < 0.005$, $****p < 0.001$ (between conditions); $\#p < 0.05$, $\#\#p < 0.01$, $\#\#\#p < 0.005$, $\#\#\#\#p < 0.001$ (within the same condition across days).

Fig. S12 Cytokine levels in supernatants under different culture conditions, including co-culture with RBCs or RBC-EVs, on day 5. (a–d) Concentrations of IL-8, MIP-1α, RANTES, and MCP-1 under different conditions. **(e–h)** Concentrations of the same cytokines after co-culture

with nRBCs or pRBCs under ±FBS/+PMA conditions. **(i–l)** Cytokine levels after co-culture with nRBC-EVs or pRBC-EVs under ±FBS/+PMA conditions. Statistical significance: *$p < 0.05$, **$p < 0.01$, ***$p < 0.005$, ****$p < 0.001$.

Table 1. List of primer sequences used for the qPCR analysis

Gene	Forward (5'-3')	Reverse (5'-3')
Human *Gapdh*	ACTGCCACCCAGAAGACTGT	CCATGCCAGTGAGCTTCC
Human *Notch-3*	TGCCTGTCTTCCTGGGT	AGCGTGTTGAAGCAGGTA
Human *Dll-4*	TCATTGCCACGGAGGT	CAAAGGTGTGGAAGGGTA
Human *PDGFR-β*	AAGAAAGTGGGCGGCT	CGGTGATGTTGATGGCA
Human *Bax*	TCAGGATGCGTCCACCAAGAAG	TGTGTCCACGGCGGCAATCATC
Human *Bcl-2*	ATCGCCCTGTGGATGACTGAGT	GCCAGGAGAAATCAAACAGAGGC
Human *Caspase-3*	GGAAGCGAATCAATGGACTCTGG	GCATCGACATCTGTACCAGACC
Human *Caspase-9*	GTTTGAGGACCTTCGACCAGCT	CAACGTACCAGGAGCCACTCTT
Human *Atg-7*	CGTTGCCCACAGCATCATCTTC	CACTGAGGTTCACCATCCTTGG
Human *mTOR*	AGCATCGGATGCTTAGGAGTGG	CAGCCAGTCATCTTTGGAGACC

Human *Nox-1*	GGTTTTACCGCTCCCAGCAGAA	CTTCCATGCTGAAGCCACGCTT